Organic & Biomolecular Chemistry

PAPER

View Article Online
View Journal | View Issue

Cite this: *Org. Biomol. Chem.*, 2014, **12**, 2675

Comparison of alternative nucleophiles for Sortase A-mediated bioconjugation and application in neuronal cell labelling†

Samuel Baer,[a] Julie Nigro,[a,b] Mariusz P. Madej,[a] Rebecca M. Nisbet,[a,b] Randy Suryadinata,[a] Gregory Coia,[a] Lisa P. T. Hong,[a] Timothy E. Adams,[a] Charlotte C. Williams*‡[a] and Stewart D. Nuttall‡[a,b]

The Sortase A (SrtA) enzyme from *Staphylococcus aureus* catalyses covalent attachment of protein substrates to pentaglycine cross-bridges in the Gram positive bacterial cell wall. *In vitro* SrtA-mediated protein ligation is now an important protein engineering tool for conjugation of substrates containing the LPXTGX peptide recognition sequence to oligo-glycine nucleophiles. In order to explore the use of alternative nucleophiles in this system, five different rhodamine-labelled compounds, with N-terminal nucleophilic amino acids, triglycine, glycine, and lysine, or N-terminal non-amino acid nucleophiles ethylenediamine and cadaverine, were synthesized. These compounds were tested for their relative abilities to function as nucleophiles in SrtA-mediated bioconjugation reactions. N-Terminal triglycine, glycine and ethylenediamine were all efficient in labelling a range of LPETGG containing recombinant antibody and scaffold proteins and peptides, while reduced activity was observed for the other nucleophiles across the range of proteins and peptides studied. Expansion of the range of available nucleophiles which can be utilised in SrtA-mediated bioconjugation expands the range of potential applications for this technology. As a demonstration of the utility of this system, SrtA coupling was used to conjugate the triglycine rhodamine-labelled nucleophile to the C-terminus of an Im7 scaffold protein displaying Aβ, a neurologically important peptide implicated in Alzheimer's disease. Purified, labelled protein showed Aβ-specific targeting to mammalian neuronal cells. Demonstration of targeting neuronal cells with a chimeric protein illustrates the power of this system, and suggests that SrtA-mediated direct cell-surface labelling and visualisation is an achievable goal.

Received 21st November 2013,
Accepted 3rd March 2014

DOI: 10.1039/c3ob42325e

www.rsc.org/obc

Introduction

Precise, reliable, and reproducible conjugation of chemical substances to proteins is a long-held goal of the chemistry–biology research community.[1,2] For example, chemical and biological conjugation of small molecule cytotoxic drugs or imaging agents to monoclonal antibodies and their recombinant fragments, to form antibody-drug conjugates (ADCs), is an expanding area of study and commercial interest.[3,4] A drawback in many ADCs reported to date is the inability to precisely conjugate agents to specific residues or domains on the antibody molecule without impacting activity or pharmacokinetics,[2] giving rise to heterogeneous mixtures as conjugation generally occurs at a number of sites on the antibody.[5] For example, the covalent attachment of the cytotoxic maytansinoid, (DM1), to the anti-ErbB2 monoclonal antibody trastuzumab, an ADC referred to as T-DM1, which is approved for the treatment of metastatic breast cancer.[5,6] DM1 is introduced to lysine-amine residues on trastuzumab through a linker, giving a heterogeneous mixture with an average of 3.5 DM1 molecules per trastuzumab molecule.[5]

An alternative to chemical conjugation is to use biological means, for example, the Sortase family of enzymes.[7,8] Sortases have evolved in Gram positive bacteria as a mechanism of generic, yet precise and efficient, covalent attachment of proteins (including virulence factors) to the outer cell wall.[9] Sortase A (SrtA), the first member of the family to be described, is an integral membrane protein attached to the outer surface of the bacterial cell[10] where it accepts proteins exported through the secretory apparatus tagged with an ^{N}LPETGX^{C} (or equivalent) motif. The enzyme then covalently couples the C-terminus of the target protein to the free

[a]*CSIRO Materials Science and Engineering, 343 Royal Parade, Parkville, Victoria 3052, Australia. E-mail: Charlotte.Williams@csiro.au*
[b]*Preventative Health Flagship, 343 Royal Parade, Parkville, Victoria 3052, Australia*
†Electronic supplementary information (ESI) available: Further experimental details for expression and purification of SrtA and conjugation optimisation and time-course reactions. See DOI: 10.1039/c3ob42325e
‡These authors contributed equally to the manuscript.

N-terminus of the abundant poly-glycine acceptor peptides located on and within the thick peptidoglycan matrix.[11,12] Further variants of Sortase (B, C, D isoforms) are implicated in specialized functions such as pilus growth and attachment, and sporulation.[9,10,13] Unsurprisingly, this robust natural protein ligation system has been eagerly embraced by the biotechnology community and many applications have been described in the protein engineering and bioconjugation fields[14,15] including but 'by no means limited to' recent advances in protein circularisation,[16] antibody functionalisation[17] and half-life extension.[18]

When the target LPXTGX recognition sequence is within the SrtA active site, it is subjected to nucleophilic attack by a thiol, from cysteine184, a residue which is highly conserved across the Sortase family.[12] This attack at the carbonyl of the Thr-Gly bond, results in the formation of a short-lived tetrahedral oxyanion transition state that is stabilised by a hydrogen bond with arginine197.[15] Subsequent protonation of the leaving group (Gly-X) leads to formation of an acyl-enzyme intermediate. The acyl-enzyme intermediate then faces nucleophilic attack at the threonine carbonyl, forming a new amide bond and releasing the Sortase-Cys. It is this last nucleophilic attack that is the focus of this work. The N-terminal nucleophile is an amino-group, usually from a terminal glycine residue. Interestingly, there have been divergent observations reported regarding the rules for this amino-group to act as an effective nucleophile and the potential for non-glycine peptide or non-peptide nucleophilic activity.[19–21] For example, N-terminal glycine analogues such as alanine have appeared to be ineffective[22] as are non-peptide, non-amine nucleophiles such as dithiothreitol (DTT) or beta-mercaptoethanol (BME).[19] A second amide bond after the C-terminal Gly-carbonyl seems to be required[19] and it is generally assumed that there must be at least one N-terminal glycine, although two or more have been reported as 'optimal'.[23] Substitution of alanine and valine following the first glycine have been reported as not as efficient as glycine.[24] Complicating factors include the possible reversibility of the reaction with competition from the cleaved and released glycine from LPETGX[22] and the requirement for a minimal length of flexible peptide to ensure steric access to the enzyme active site and N-terminal amine accessibility.

In order to further elucidate substrate requirements in this last nucleophilic attack, we describe a series of experiments aimed at exploring alternative nucleophiles for use in the SrtA system. We successfully demonstrate that triglycine, glycine and ethylenediamine are efficient nucleophiles with respect to SrtA-mediated labelling of a range of recombinant antibody and scaffold proteins and peptides that contain the LPETGG recognition sequence, and further demonstrate the utility of this system in Aβ-mediated labelling of primary neuronal cultures.

Results

Comparison of five SrtA nucleophiles

A linear sequence consisting of 3–5 consecutive glycine residues is well-established as required for efficient nucleophilic reactivity for *in vitro* SrtA bioconjugation reactions. To compare alternative nucleophiles, we synthesised five rhodamine (5/6-carboxytetramethylrhodamine, TAMRA) functionalised compounds: TAMRA-EDA-triglycine; TAMRA-EDA-glycine; TAMRA-EDA-lysine; TAMRA-EDA; and TAMRA-cadaverine (Fig. 1; EDA = ethylenediamine). The five variants were isolated in high purity and characterised by ES-MS and analytical HPLC. The triglycine nucleophile (TAMRA-EDA-triglycine) was

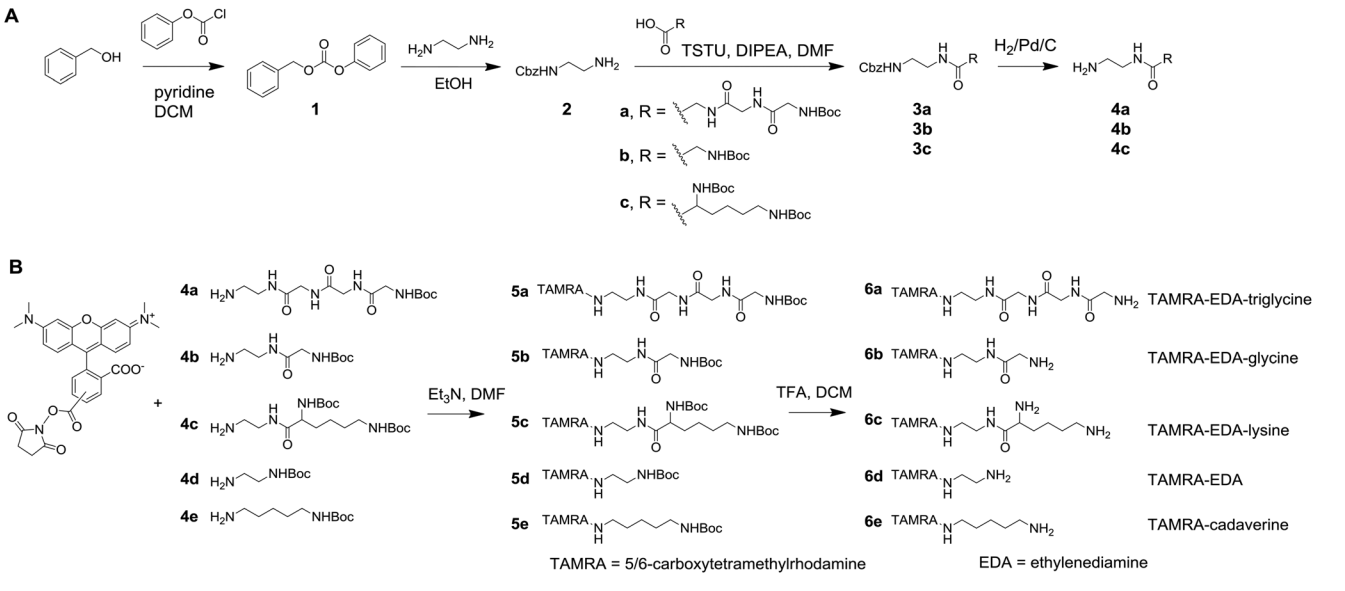

Fig. 1 Synthesis of Rhodamine-labelled nucleophiles **6a–e**. (A) Synthetic route to prepare amine functionalised, *N*-Boc-protected amino acids and (B) Synthetic route to prepare rhodamine-labelled nucleophiles. Dichloromethane (DCM), ethanol (EtOH), *N*,*N*,*N*′,*N*′-tetramethyl-*O*-(*N*-succinimidyl)-uronium tetrafluoroborate (TSTU), diisopropylethylamine (DIPEA), dimethylformamide (DMF), triethylamine (Et_3N), trifluoroacetic acid (TFA).

chosen as a positive control for SrtA-mediated conjugation and the single terminal glycine nucleophile (TAMRA-EDA-glycine) was investigated in order to clarify conflicting reports regarding the ability of a single glycine to act as an effective nucleophile. Understanding the efficiency of a single terminal glycine to act as a nucleophile in SrtA-mediated conjugations is an important factor considering the possible reversibility of the reaction with competition from the cleaved and released glycine from LPETGX.[22] Two different length, non-amino acid nucleophiles were chosen, ethylenediamine (1,2-diaminoethane) and cadaverine (1,5-diaminopentane), which contain an N-terminal nucleophilic primary amine. Understanding the efficiency of (and selectivity between) non-amino acid nucleophiles, of similar size and structure to the amino acid terminal nucleophiles, will aid in understanding the mechanism of SrtA-mediated ligation. All five compounds were tested for nucleophilic efficiency in SrtA-mediated bioconjugation reactions in our model system where an LPETGG acceptor sequence is positioned between the N-terminal Im7 4-helical scaffold protein[25] and C-terminal dual FLAG affinity tags and associated linker sequences. Successful addition of rhodamine to the Im7 protein was measured both as a decrease in protein molecular weight (due to loss of the FLAG epitopes; ~2.4 kDa) and rhodamine fluorescence measured at 605 nm. Both triglycine (as expected) and glycine alone acted as nucleophiles, and a significant signal was also observed for ethylenediamine (Fig. 2). In these assays, a band representing the Im7-LPET/SrtA reaction intermediate (SrtA + Im7) was clearly visible at ~29 kDa (as well as dimers of SrtA) which dissociated upon nucleophilic attack. Importantly, the Im7-rhodamine end products (Im7-LPET-TAMRA) for the TAMRA-EDA-triglycine and TAMRA-EDA-glycine reactions were also characterised by Electrospray ionization mass spectrometry, ESI-MS (Fig. 3D and E). The Im7-LPET/SrtA reaction intermediate was also detected by mass spectrometry for the TAMRA-EDA-lysine, TAMRA-ethylenediamine and TAMRA-cadaverine reactions, (Fig. 3F–H). The presence of greater amounts of this intermediate for the TAMRA-EDA-lysine, TAMRA-ethylenediamine and TAMRA-cadaverine reactions, while not quantitative, indicates that due to poor nucleophilic attack these intermediates were not dissociated, leading to lower amounts of product for this particular protein. Prior to further experimentation, this system was optimised with regard to nucleophile and SrtA concentrations (Fig. S1†), consistent with our previously reported results,[26] and confirmation was obtained that the SrtA-mediated labelling was specific for the LPETGG recognition sequence (Fig. S2†).

To demonstrate that the results obtained were not confined to the Im7 system, a series of experiments was performed utilising a range of LPETGG-tagged acceptor proteins, including: a recombinant antibody Fab fragment (52 kDa); a recombinant scFv antibody (29 kDa),[26] the Im7 protein displaying the amyloid beta ($A\beta_{1-42}$) peptide at the N-terminus (17 kDa); the Im7 protein alone (12 kDa); and a 23 residue peptide consisting of $A\beta_{1-16}$ + LPETGG (2.6 kDa) (Fig. 4A and E). In all cases, glycine alone was as efficient a nucleophile as triglycine and

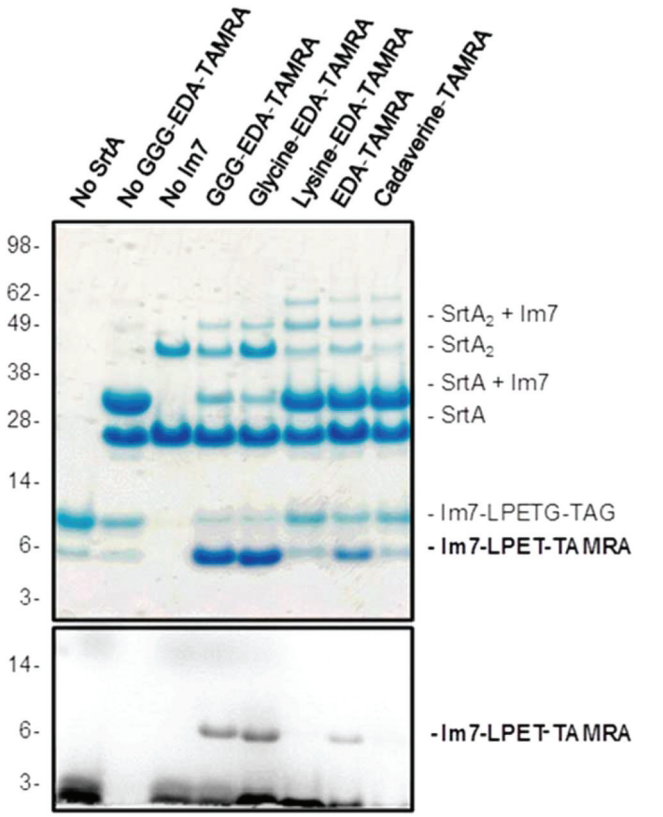

Fig. 2 Five rhodamine-labelled compounds were tested for their ability to act as nucleophiles in SrtA-mediated bioconjugation reactions utilising C-terminally LPETGG & dual-FLAG epitope-tagged Im7 protein. The decrease in molecular weight associated with replacement of the FLAG epitopes by rhodamine is clearly observed (top panel, Coomassie stained non-reducing SDS-PAGE), which is reflected by the associated gain in fluorescence (bottom panel, measured at 605 nm). Various intermediates and SrtA dimeric species are visible at higher molecular weights (SrtA + Im7: intermediate species prior to nucleophilic attack; $SrtA_2$: dimer of SrtA; $SrtA_2$ + Im7 intermediate species consisting of SrtA dimer + Im7 prior to nucleophilic attack). Approximate molecular weights (kDa) are indicated to the left. Fluorescent bands at the bottom of the gel (bottom panel, <3 kDa) are due to excess, unreacted rhodamine-labelled compound.

clear activity was also observed for ethylenediamine. Interestingly, for these additional examples, and in particular for the two larger proteins (Fab and scFv), a modest but consistent labelling was observed for both lysine and cadaverine, suggesting at least a minimal ability of these two compounds to act as nucleophiles in these systems (Fig. 4A and B). 1,5-Diaminopentane (cadaverine) has been reported to act as an efficient nucleophilic acyl-acceptor in SrtA-mediated conjugation reactions, upon extended incubation either with an LPXTG containing nonapeptide (9 h) or an LPETG containing glycosyltransferase (overnight).[20] This cadaverine nucleophile is a biotin-labelled 1,5-diaminopentane and successful conjugations were determined by detection of product by MALDI-MS for the short peptide, and by immunoblotting with streptavidin–HRP for the glycosyltransferase conjugation.[20] In order to further investigate whether extended incubation of

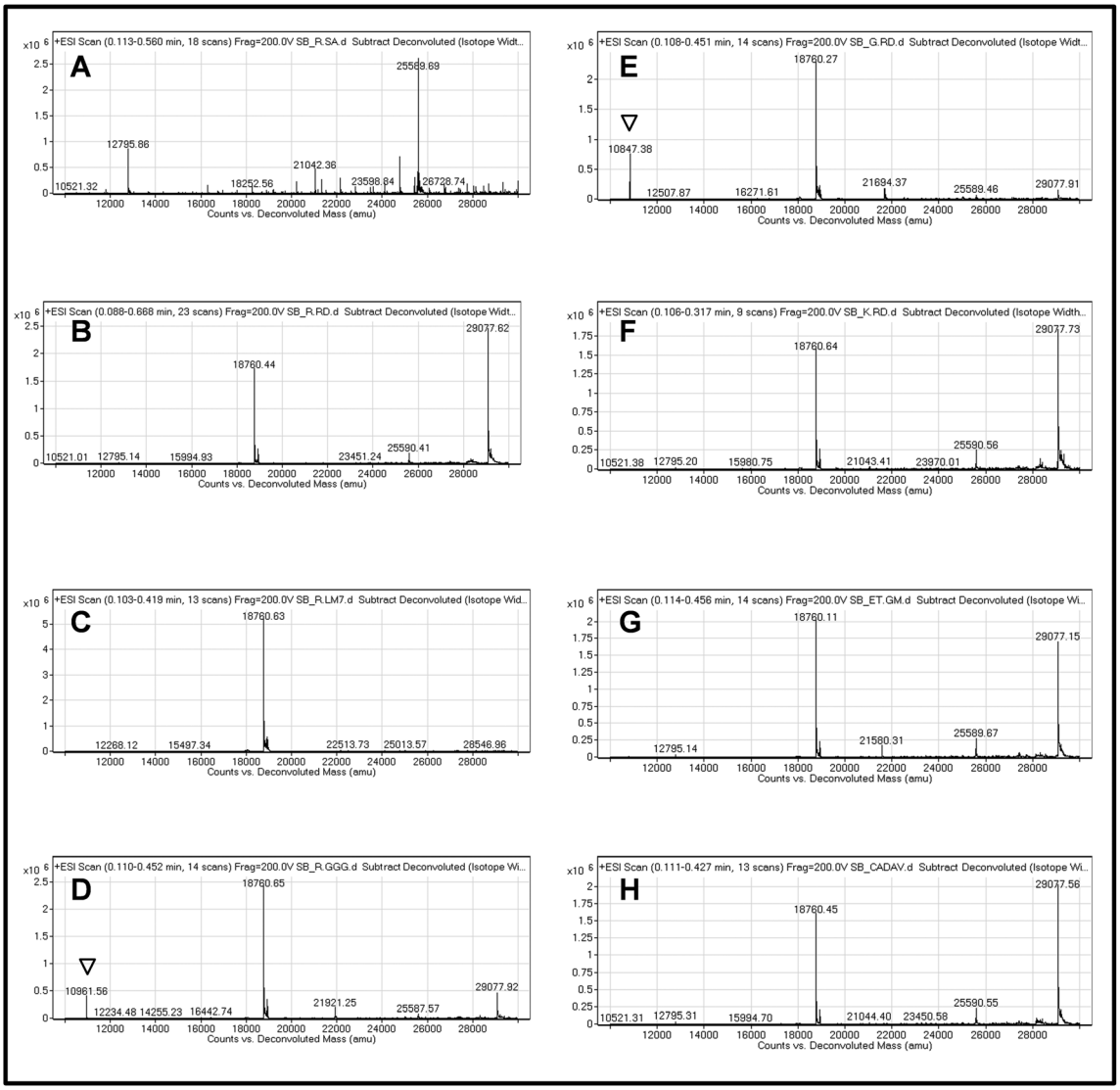

Fig. 3 Electrospray ionization (ESI+) Mass Spectra of reaction mixtures corresponding to lanes 1–8 from Fig. 2B. (A) No SrtA; (B) No TAMRA-EDA-GGG; (C) no Im7; (D) TAMRA-EDA-GGG; (E) TAMRA-EDA-glycine; (F) TAMRA-EDA-lysine; (G) TAMRA-EDA; and (H) TAMRA-cadaverine-; (EDA = ethylenediamine; TAMRA = 5/6-carboxytetramethylrhodamine). Arrows in panels D and E represent predicted molecular masses for rhodamine-labelled Im7 conjugates using triglycine and glycine nucleophiles respectively. While a rhodamine-labelled product is faintly visible for TAMRA-EDA by fluorescence (Fig. 1B, bottom panel), it is not detected by mass spectrometry. SrtA is present at 18.760 kDa in all spectra except for panel A, which is a SrtA free control. The species at ~29 kDa represents an intermediate complex of Im7-LPETGG and SrtA enzyme prior to nucleophilic attack (Im7-LPET/SrtA).

our TAMRA-cadaverine nucleophile would promote more efficient labelling, we extended reaction periods to 5 and 24 hours, for both the Im7 system (which showed the poorest reactivity for this nucleophile) and for the scFv antibody. For use in these extended reaction timed experiments, Im7-LPETGG was purified to high yields through a C-terminal hexahistidine tag (replacing the dual FLAG epitopes). Results for the scFv conjugation reaction over extended reaction times, confirmed the abilities of lysine and cadaverine to act as nucleophiles (Fig. S3A†). However, in the case of Im7-LPETGG only the most barely detectable activity was observed (by fluorescence overexposure) (Fig. S3B†). Incubation time beyond 3 hours did not result in an increased yield of product. This is in contrast with the ability of the cadaverine-based acyl-acceptor reported by Ito *et al.* to act as an effective nucleophile in SrtA-mediated conjugation reactions with the LPXTG-labelled peptide and protein reported by these workers.[20] Thus, we conclude that reaction of the nucleophile appears to be greatly dependent upon the LPXTG-labelled peptide or protein that is being used in the SrtA-mediated conjugation reactions. This is evident within our own work and in comparison with others, which suggests the mechanism of nucleophilic attack of the protein-LPXT-SrtA intermediate is dependant not only on the nature of the nucleophile but on the nature of the protein containing the LPXTGX recognition sequence.

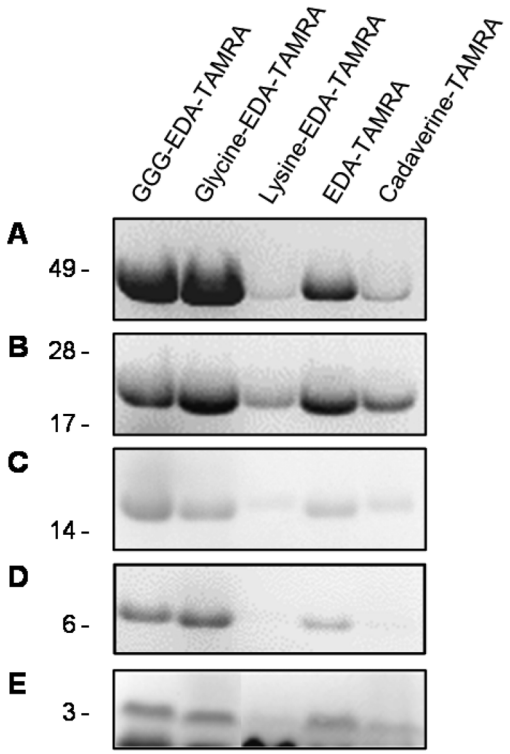

Fig. 4 Image of SDS-PAGE gel (measured at 605 nm, to detect fluorescence) of SrtA-mediated labelling reactions utilizing C-terminally LPETGG-tagged proteins. (A) Antibody Fab fragment 39S-3. (B) Antibody scFv fragment 38B-5. (C) The Im7 protein displaying $A\beta_{1-42}$ peptide at the N-terminus. (D) The Im7 protein. (E) $A\beta_{1-16}$-LPETGG peptide.

SrtA-mediated labelling of Aβ peptide and neuronal cell imaging

The $A\beta_{1-42}$ peptide is recognised as a key molecule in the aetiology of Alzheimer's disease, through its ability to interfere with neuronal function, as well as induce an inflammatory response after aggregation into amyloid plaques.[27,28] To demonstrate an application of the rhodamine-based SrtA-mediated bioconjugation system, the Im7 scaffold protein was protein-engineered to display $A\beta_{1-42}$ at the N-terminus (Fig. 5A). Aβ-Im7-LPETGG, Im7-LPETGG and Im7 (no LPETGG sequence) proteins were labelled with rhodamine *via* SrtA-mediated conjugation reactions with TAMRA-EDA-GGG, and were assessed for fluorescence. As expected, native Im7 with no SrtA recognition sequence was not labelled (indicating the absence of non-specific interactions), while both Im7-LPETGG and $A\beta_{1-42}$-LPETGG were efficiently labelled, with only small amount of unreacted protein and Im7-LPET/SrtA intermediate apparent in the reaction mixture (Fig. 5B). Prior to cell studies, non-reacting components were removed by immunoprecipitation using Ni^{2+}-Sepharose (to remove SrtA) and anti-FLAG-Sepharose beads (to remove Im7 and $A\beta_{1-42}$-Im7), taking advantage of the loss of the FLAG epitopes from the protein scaffold upon rhodamine addition in this system. Upon addition of labelled proteins to fixed murine primary neuronal cultures, only very weak binding was observed for the Im7-LPETG-rhodamine as expected (Fig. 5D–F). In contrast, $A\beta_{1-42}$-Im7-LPETG-rhodamine bound strongly to the cell body (including the cell membrane of this region) and nucleoli of fixed neuronal cultures (Fig. 5G–I).

Discussion

We have demonstrated that N-terminal triglycine, glycine and ethylenediamine labelled with the fluorescent dye rhodamine are capable of acting as effective nucleophiles for bioconjugation to a range of recombinant antibody constructs and peptides. In exploring the reactivity of these terminal amines we have progressed our understanding of the requirements for the enzyme-recognition sequences for SrtA-mediated ligations. Specifically, our findings can be reconciled with previous work as follows: (i) The Gram positive cell wall contains pentaglycine bridges as the naturally evolved nucleophile for SrtA conjugation and it is therefore unsurprising that the enzyme demonstrates maximal activity for this configuration. (ii) Evolution of different Sortase variants with altered recognition sequences suggests a degree of flexibility in the system. For example, in SrtD-mediated pilin assembly the ε-amino group of lysine within the YPKN motif initiates nucleophilic attack,[29] while SrtB from *Bacillus anthracis* accepts *meso*-diaminopimelic acid as a nucleophile.[30] (iii) There is also clearly further potential for nucleophile heterogeneity, with reports of transfer to kanamycin and oligosaccharides.[31] (iv) Our demonstration of marginal activity for both lysine and cadaverine in our SrtA-based systems suggests that any promiscuity in nucleophilic utilisation is probably tightly controlled in biological systems, in line with the distinction between household (SrtA) and more tightly regulated (SrtB-D) isoforms and the nature of these tightly controlled biological processes.

This study of the nucleophilic efficiency of different N-terminal amino-groups using different amino-acid, and different length non-amino acid, nucleophiles in SrtA-mediated conjugations has led to some interesting outcomes. A single N-terminal glycine is not always reported as an effective nucleophile;[19,22] in our system it is equally as effective as triglycine which is widely accepted as a good substrate. This result is significant given the possible reversibility of the SrtA reaction, because the terminal glycine residue is cleaved and released from the LPETGX sequence; this is now able to compete with the nucleophile for reaction at the threonine of the LPET-SrtA intermediate. In our work, the non-glycine peptide, that is N-terminal lysine, showed some, but limited overall effective nucleophilic activity which may suggest unfavourable steric bulk in the SrtA active site. The difference in ability of the non-peptide terminal amines (ethylenediamine and cadaverine) to work as nucleophiles in Sortase reactions alludes to a size-specific nucleophilic active site. Terminal ethylenediamine (1,2-diaminoethane) worked well as a nucleophile whereas cadaverine (1,5-diaminopentane), which is only three carbon atoms longer, generally led to

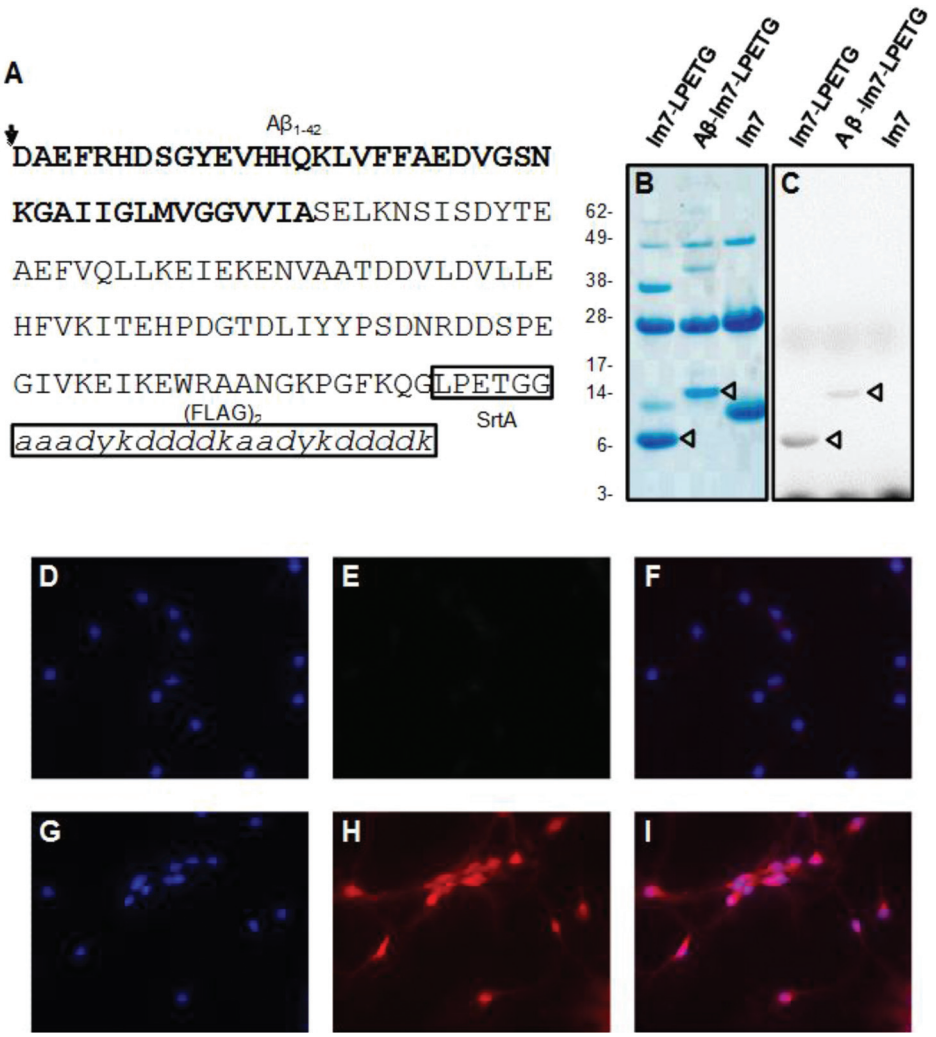

Fig. 5 Neuronal cell imaging by rhodamine-labelled proteins. (A) The Im7 protein encodes C-terminal FLAG affinity and SrtA tags for affinity purification and labelling respectively. The $A\beta_{1-42}$ peptide is displayed at the scaffold's N-terminus, where it is precisely N-terminally processed (arrow) during protein production. (B) Coomassie stained non-reducing SDS-PAGE gel. (C) Image of the same gel in B measured at 605 nm, to detect fluorescence. (B–C) Im7-LPETGG and $A\beta_{1-42}$-LPETGG are labelled with rhodamine using TAMRA-EDA-GGG (arrowed), but wild type Im7 which lacks an LPETGG sequence is not. In this reaction (prior to affinity purification) the bands at ~26- and ~47-kDa represent SrtA and SrtA dimer respectively; intermediate products (Im7-LPET/SrtA) are also present for Im7-LPETG and $A\beta_{1-42}$-LPETG as described for Fig. 2. Only the final Im7-LPET-rhodamine and $A\beta_{1-42}$-Im7-LPET-rhodamine products are visible by fluorescence. (D–F) Im7-LPET-rhodamine binding to fixed murine primary neuronal cultures. (G–I) $A\beta_{1-42}$-Im7-LPET-rhodamine binding to fixed murine primary neuronal cultures. D and G show DAPI staining only; E and H show rhodamine staining only. F is the merged micrograph of D and E. I is the merged micrograph of G and H. Micrographs are 40× magnification.

lesser amounts of conjugate. Nucleophilic efficiency of ethylenediamine in SrtA-mediated conjugations suggests promiscuity in the SrtA active site, thus allowing for nucleophilic attack without site specific recognition of an amino acid sequence. The ability of ethylenediamine to function as a nucleophile in our SrtA-mediated conjugations also contradicts the traditional rules for SrtA nucleophiles that allude to the requirement for an N-terminal glycine. The mechanism of SrtA-mediated conjugations, and in particular of nucleophilic attack is clearly a complex one that potentially involves a size/shape-specific nucleophilic active site as well as other potential considerations such as pK_a of the nucleophiles, which has not been addressed here but is a potential contributor to this mechanism.

The results we have presented are qualitative rather than strictly quantitative, due to the difficulty of accurately quantitating precise yield figures within acceptable levels of error in gel fluorescence and by mass spectrometry. This is compounded by the downstream processes required for protein purification including immune-pull-down and gel filtration which result in progressive losses. However, as an example at the conclusion of these procedures a recovery yield of 15–20% purified labelled protein is not uncommon in our hands. Additionally, by presenting relative labelling levels for five different proteins/peptides we provide a basis for direct comparison between all five nucleophiles across a range of LPETGG substrates.

This work has also initiated further systematic and comprehensive studies involving the use of a range of amino acid and non-amino acid based nucleophiles for SrtA-mediated conjugation, which will be reported in due course. These further studies will include considerations for the role that potential differences in pK_a of each of the terminal nucleophilic amino groups for each of the nucleophiles may play in the efficiency of conjugation reactions.

Beyond dissection of the workings of *in situ* bacterial structure-function, our results are useful in application of SrtA labelling technology for *in vitro* applications. Our demonstration that lysine and cadaverine activity appeared dependent upon the target protein scaffold, with more significant conjugation observed for the two larger test proteins (Fab and scFv antibody fragments) than for the helical Im7 scaffold, is a significant consideration for planning of bioconjugation experiments; and suggests that variations may occur, dependent not only upon the specific Sortase recognition signal and nucleophilic composition, but also upon the nature and size of the target protein. Obviously, steric considerations for access to the enzyme active site are of concern and the differences observed for our constructs may not necessarily be apparent for more extended *i.e.*, pentaglycine, nucleophiles. Our previous work demonstrated site-specific ligation of small molecule GGG constructs to the therapeutically relevant sc528 scFv without compromising the ability to bind antigen with high affinity.[26] The present study utilised the more chemically and biologically tractable fluorophore rhodamine, which displays photostability across a pH range, and good fluorescence intensity with a narrow red emission spectrum.

As an example of this technology, we demonstrated successful labelling of a protein scaffold in the presence and absence of Aβ peptide and measured binding to fixed primary neuronal cells cultured from mouse brain. The binding of Aβ to the cell membrane of live cells has been reported previously,[32,33] however, we utilised acetone-fixed cells which not only cross-links the cellular structures but also permeabilises the cell membrane. Hence, in our study the $A\beta_{1-42}$-Im7-LPET-rhodamine bound to the cell membrane and the cell body, suggesting widespread localisation of the Aβ peptide, consistent with previous reports.[34,35] The binding of Aβ to nucleoli has not been reported and our data may reflect the interaction of Aβ with ribosomal proteins in this region.[36] These results demonstrate not only the utility of our SrtA-mediated rhodamine labelling, but also represent a promising system for investigation of compounds which interfere with Aβ-mediated cellular binding and possibly neuronal toxicity.

Conclusion

SrtA-mediated protein ligation represents a precise, reliable and reproducible tool for functionalisation of biologically important molecules. Expansion of the range of available nucleophiles which can be utilised in such bioconjugation systems extends the range of potential applications for this technology, for example the ability to reduce the nucleophile to a single N-terminal glycine (or ethylenediamine) is of value in situations where the introduced sequence, post-conjugation, is to be minimised. This study has progressed the understanding regarding determination of the nucleophilic specificity, for both amino acid and non-amino acid nucleophilic compounds, in SrtA-mediated conjugations, which ultimately will lead to a better understanding of the nucleophilic binding site in the enzyme. Not only does the nature of the nucleophile determine efficiency of SrtA-mediated conjugation, but the nature and size of the target LPXTG-labelled protein also plays a key role in reaction efficiency. The demonstration of targeting of neuronal cells with a Sortase-labelled medically important peptide–protein–rhodamine conjugate illustrates the power of this system and further suggests that direct SrtA-mediated cell-surface labelling and visualisation may be an achievable goal.

Experimental

Cloning, expression, and purification of SrtA

A DNA cassette encoding residues 60–208 of the *S. aureus* SrtA was synthesised at Geneart AG (Regensburg, Germany, http://www.geneart.com) in the expression vector pET28a (Novagen). The sequence included 5′ *Nde*I and 3′ *Bam*H1 sites and initiating methionine and N-terminal hexahistidine tag sequences.[26] Details of pET28a–SrtA protein expression are described in the ESI.†

Synthesis of nucleophiles

General. All chemicals were used as received (Aldrich), NHS-rhodamine (5/6-carboxytetramethylrhodamine succinimidyl ester, 5/6-TAMRA SE) was purchased from Thermo Scientific. NMR spectra were recorded with a Bruker ARX-400 spectrometer at ambient temperature and were referenced with respect to residual solvent peaks in deuterated solvents. Electrospray ionization (ESI) mass spectra were recorded on an Applied Biosystems API 150EX mass spectrometer. *N*-Boc glycine was purchased from Aldrich, *N*-Boc-GGG[37] and diBoc-lysine[38] were prepared by modifications of published procedures.

*Benzylphenylcarbonate (**1**).* To a stirred solution of benzyl-alcohol (500 μL, 4.83 mmol) and pyridine (470 μL, 5.82 mmol) in dichloromethane (DCM, 30 mL) was added drop wise, phenylchloroformate (730 μL, 5.82 mmol). The solution was stirred at room temperature under nitrogen for 16 h. The reaction mixture was washed with H_2O, then 2 M H_2SO_4, and the organic layer was dried ($MgSO_4$), filtered and concentrated under reduced pressure to give crude benzylphenylcarbonate (**1**) as a pale tan colored oil (1.10 g, quantitative yield). δ_H (400 MHz, CD_3OD) 7.40–7.15 (m, 10H, Ar*H* × 10), 5.25 (s, 2H, ArCH_2).

*Mono-Cbz-ethylenediamine (**2**).* A solution of benzylphenylcarbonate (1.10 g, 4.83 mmol) and ethylenediamine (290 mg, 4.83 mmol) in ethanol (EtOH, 30 mL) was stirred at room

temperature under nitrogen for 16 h. The reaction mixture was concentrated under reduced pressure then dissolved in H_2O (25 mL). The solution was acidified to pH 3 using 5% HCl (2 mL) and extracted into DCM (2 × 50 mL). The aqueous layer was made alkaline by 1 M NaOH (2 mL) and extracted into DCM (3 × 60 mL), dried ($MgSO_4$), filtered and concentrated under reduced pressure to give mono-Cbz-ethylenediamine (**2**) as a pale tan colored oil (332 mg, 28% yield calculated from **1**). δ_H (400 MHz, $CDCl_3$) 7.38–7.27 (m, 5H, Ar*H* × 5), 5.11 (s, 2H, Ar*CH*$_2$), 3.24 (t, *J* 6.0 Hz, 2H, NH*CH*$_2$), 2.83 (t, *J* 6.0 Hz, 2H, *CH*$_2$NH$_2$).

General procedure for mono-Cbz-ethylenediamine-amino acids (3). To a stirred solution of *N*-Boc protected amino acid (1 eq.) in DMF (2.0 mL) was added diisopropylethylamine (DIPEA, 5 eq.) followed by a solution of *N*,*N*,*N*′,*N*′-tetramethyl-*O*-(*N*-succinimidyl)uronium tetrafluoroborate (TSTU, 1.3 eq.) in DMF (2.0 mL). The solution was stirred at room temperature, under nitrogen for 30 min. mono-Cbz-ethylenediamine (**2**, 1.4 eq.) was added as a solution in DMF (2.0 mL) and the solution stirred for a further 16 h. The reaction mixture was concentrated under reduced pressure to yield crude mono-Cbz-ethylenediamine-amino acid (**3**). The residue was taken up into 1 : 1 MeOH–H_2O [20 mg mL^{-1}] and filtered through a 0.45 μm Acrodisc for purification by reverse phase HPLC. HPLC conditions: 0.1% TFA, 20–80% MeCN from 2–26 min, flow 10 mL min^{-1}, λ = 214 nm, ambient temperature.

*Cbz-NH-(CH$_2$)$_2$-NH-GGG-NH-Boc (**3a**).* HPLC purification revealed a major peak at R_t 15.7 min, giving Cbz-NH-(CH$_2$)$_2$-NH-GGG-NH-Boc (**3a**) as a colourless oil (80.0 mg, 50%). δ_H (400 MHz, CD_3OD) 7.31–7.28 (m, 5H, Ar*H* × 5), 5.07 (s, 2H, Ar*CH*$_2$), 3.88 (s, 2H, G-*CH*$_2$), 3.83 (s, 2H, G-*CH*$_2$), 3.73 (s, 2H, G-*CH*$_2$), 3.27 (t, *J* 6.0 Hz, 2H, NH*CH*$_2$), 3.25 (t, *J* 6.0 Hz, 2H, *CH*$_2$NH), 1.44 (s, 9H, Boc). *m*/*z* (ESI) found 466.3 (M^+ + 1), calculated 465.51.

*Cbz-NH-(CH$_2$)$_2$-NH-glycine-NH-Boc (**3b**).* HPLC purification revealed a major peak at R_t 18.1 min, yielding Cbz-NH-(CH$_2$)$_2$-NH-glycine-NH-Boc (**3b**) as a colourless oil (38.0 mg, 95%). δ_H (400 MHz, CD_3OD) 7.34–7.28 (m, 5H, Ar*H* × 5), 5.07 (s, 2H, Ar*CH*$_2$), 3.66 (s, 2H, G-*CH*$_2$), 3.31 (t, *J* 5.8 Hz, 2H, NH*CH*$_2$), 3.23 (t, *J* 5.8 Hz, 2H, *CH*$_2$NH), 1.44 (s, 9H, Boc). *m*/*z* (ESI) found 352.5 (M^+ + 1), calculated 351.40.

*Cbz-NH-(CH$_2$)$_2$-NH-lysine-NH-Boc (**3c**).* HPLC purification revealed a major peak at R_t 23.3 min, isolating Cbz-NH-(CH$_2$)$_2$-NH-lysine-NH-Boc (**3c**) as a colourless oil (67.5 mg, 89%). δ_H (400 MHz, CD_3OD) 7.35–7.28 (m, 5H, Ar*H* × 5), 5.07 (s, 2H, Ar*CH*$_2$), 3.94 (t, *J* 5.6 Hz, 1H, C*H*), 3.30 (t, *J* 6.2 Hz, 2H, NH*CH*$_2$), 3.22 (t, *J* 6.2 Hz, 2H, *CH*$_2$NH), 1.70 (m, 8H, *CH*$_2$ × 4) 1.43 (s, 18H, Boc × 2). *m*/*z* (ESI) found 523.6 (M^+ + 1), calculated 522.63.

General procedure for ethylenediamine-amino acids (4). A solution of mono-Cbz-ethylenediamine-amino acid (**3**) in methanol [0.1 M] was subjected to Cbz-deprotection using H-cube flow instrument (1 mL min^{-1}, 50 °C, H_2 (1 bar), 10% Pd/C) and concentrated under reduced pressure to yield ethylenediamine-amino acid (**4**).

*NH$_2$-(CH$_2$)$_2$-NH-GGG-NH-Boc (**4a**).* Colourless oil (60.9 mg, quantitative yield), δ_H (400 MHz, CD_3OD) 3.88 (s, 2H, G-*CH*$_2$), 3.83 (s, 2H, G-*CH*$_2$), 3.73 (s, 2H, G-*CH*$_2$), 3.27 (t, *J* 6.0 Hz, 2H, NH*CH*$_2$), 3.25 (t, *J* 6.0 Hz, 2H, *CH*$_2$NH), 1.44 (s, 9H, Boc).

*NH$_2$-(CH$_2$)$_2$-NH-glycine-NH-Boc (**4b**).* Colourless oil (20.0 mg, 85%). δ_H (400 MHz, CD_3OD) 3.65 (s, 2H, G-*CH*$_2$), 3.31 (t, *J* 5.8 Hz, 2H, NH*CH*$_2$), 3.23 (t, *J* 5.8 Hz, 2H, *CH*$_2$NH), 1.42 (s, 9H, Boc).

*NH$_2$-(CH$_2$)$_2$-NH-lysine-NH-Boc (**4c**).* Colourless oil (50.0 mg, 84%). δ_H (400 MHz, CD_3OD) 3.89 (t, *J* 5.6 Hz, 1H, *CH*), 3.30 (t, *J* 6.2 Hz, 2H, NH*CH*$_2$), 3.22 (t, *J* 6.2 Hz, 2H, *CH*$_2$NH), 1.70 (m, 8H, *CH*$_2$ × 4) 1.41 (s, 9H, Boc) 1.39 (s, 9H, Boc).

General procedure for rhodamine-CONH-R-NH-Boc (5). To a stirred solution of NH$_2$-R-NH-Boc (**4**) (1.2 eq.) and triethylamine (Et_3N, 5 eq.) in DMF (3 mL) was added a solution of NHS-rhodamine (1 eq.) in DMF (1 mL). The bright pink solution was stirred at room temperature under nitrogen and protected from light, for 16 h. The reaction mixture was concentrated under reduced pressure. The residue was taken up into 1 : 1 MeOH–H_2O [20 mg mL^{-1}] and filtered through a 0.45 μm Acrodisc for purification by reverse phase HPLC. HPLC conditions: 0.1% TFA, 20–80% MeCN from 2–26 min, flow 10 mL min^{-1}. HPLC revealed the presence of rhodamine-CONH-R-NH-Boc (**5**) as two major products (two structural isomers of 5/6-carboxytetramethylrhodamine succinimidyl ester).

*Rhodamine-CONH-(CH$_2$)$_2$-NH-GGG-NH-Boc (**5a**).* HPLC purification yielded two major peaks at R_t 15.0 min and R_t 16.0 min, giving rhodamine-CONH-(CH$_2$)$_2$-NH-GGG-NH-Boc (**5a**) as a red powder (10.7 mg, quantitative yield). *m*/*z* (ESI) found 744.4 (M^+ + 1), calculated 743.81.

*Rhodamine-CONH-(CH$_2$)$_2$-NH-Glycine-NH-Boc (**5b**).* HPLC purification gave two major peaks at R_t 16.4 min and R_t 17.4 min, isolating rhodamine-CONH-(CH$_2$)$_2$-NH-glycine-NH-Boc (**5b**) as a red powder (10.3 mg, quantitative yield). *m*/*z* (ESI) found 630.6 (M^+ + 1), calculated 629.70.

*Rhodamine-CONH-(CH$_2$)$_2$-NH-Lysine-NH-Boc (**5c**).* HPLC purification yielded two major peaks at R_t 20.5 min and R_t 21.2 min, giving rhodamine-CONH-(CH$_2$)$_2$-NH-lysine-NH-Boc (**5c**) as a red powder (8.3 mg, 91%). *m*/*z* (ESI) found 801.5 (M^+ + 1), calculated 800.94.

*Rhodamine-CONH-(CH$_2$)$_2$-NH-Boc (**5d**).* HPLC purification gave two major peaks at R_t 18.3 min and R_t 19.2 min, yielding rhodamine-CONH-(CH$_2$)$_2$-NH-Boc (**5d**) as a red powder (7.3 mg, quantitative yield). *m*/*z* (ESI) found 573.5 (M^+ + 1), calculated 572.65.

*Rhodamine-CONH-(CH$_2$)$_5$-NH-Boc (**5e**).* HPLC purification gave two major peaks at R_t 20.6 min and R_t 21.1 min, isolating rhodamine-CONH-(CH$_2$)$_5$-NH-Boc (**5e**) as a red powder (11.0 mg, quantitative yield). *m*/*z* (ESI) found 615.5 (M^+ + 1), calculated 614.73.

General procedure for rhodamine-CONH-R-NH$_2$ (6). To a stirred solution of rhodamine-CONH-R-NH-Boc (**5**) (1 eq.) in DCM (2 mL) was added trifluoroacetic acid (TFA, 0.4 mL). The resulting pink solution was stirred at room temperature, protected from light, for 2 h. The solution was concentrated

under reduced pressure and the residue was taken up into 1 : 1 MeCN–H_2O (3 × 1 mL) and the volatiles removed under reduced pressure to yield rhodamine-CONH-R-NH_2 (**6**). The product was analysed by analytical reverse phase HPLC. HPLC conditions: 0.1% TFA, 0–80% MeCN from 2–34 min, flow 1 mL min^{-1}, λ = 214 nm. HPLC revealed the presence of rhodamine-CONH-R-NH_2 (**6**) as two major products (two structural isomers of 5/6-TAMRA SE).

*Rhodamine-CONH-$(CH_2)_2$-NH-GGG-NH_2 (TAMRA-EDA-GGG) (**6a**).* Analytical HPLC gave two major peaks at R_t 13.3 min and R_t 14.4 min corresponding to rhodamine-CONH-$(CH_2)_2$-NH-GGG-NH_2 (**6a**). *m*/*z* (ESI) found 644.6 (M^+ + 1), calculated 643.69.

*Rhodamine-CONH-$(CH_2)_2$-NH-glycine-NH_2 (TAMRA-EDA-glycine) (**6b**).* Analytical HPLC gave two major peaks at R_t 13.2 min and R_t 14.2 min corresponding to rhodamine-CONH-$(CH_2)_2$-NH-Glycine-NH_2 (**6b**). *m*/*z* (ESI) found 530.3 (M^+ + 1), calculated 529.59.

*Rhodamine-CONH-$(CH_2)_2$-NH-lysine-NH_2 (TAMRA-EDA-lysine) (**6c**).* Analytical HPLC gave two major peaks at R_t 13.7 min and R_t 14.7 min corresponding to rhodamine-CONH-$(CH_2)_2$-NH-Lysine-NH_2 (**6c**). *m*/*z* (ESI) found 601.4 (M^+ + 1), calculated 600.71.

*Rhodamine-CONH-$(CH_2)_2$-NH_2 (TAMRA-EDA) (**6d**).* Analytical HPLC gave two major peaks at R_t 14.0 min and R_t 15.2 min corresponding to rhodamine-CONH-$(CH_2)_2$-NH_2 (**6d**). *m*/*z* (ESI) found 473.3 (M^+ + 1), calculated 472.54.

*Rhodamine-CONH-$(CH_2)_5$-NH_2 (TAMRA-cadaverine) (**6e**).* Analytical HPLC gave two major peaks at R_t 14.5 min and R_t 15.6 min corresponding to rhodamine-CONH-$(CH_2)_5$-NH_2 (**6e**). *m*/*z* (ESI) found 515.7 (M^+ + 1), calculated 514.62.

Expression and purification of recombinant antibodies.

Recombinant Fab and scFv antibodies and Im7 scaffold protein were expressed as previously described.[39,40] Proteins were purified from the *E. coli* periplasmic fraction or cellular fraction (for Im7-LPETGG used in Fig. 5, where a single hexahistidine tag replaced the dual FLAG tags) by affinity chromatography and gel filtration, and validated by SDS-PAGE and mass spectrometry. The Aβ-LPETGG peptide (^{N}DAEFRHDSGYEVHHQKSLPETGG^C) was synthesised by Keck Biotechnology (New Haven, CT).

SrtA-mediated bioconjugation

Typical SrtA labelling reactions were performed in SrtA reaction buffer (50 mM Tris, 150 mM NaCl, 10 mM $CaCl_2$, pH 7.5). Reactions containing 20 μM recombinant protein, 2 mM nucleophile-rhodamine and 60 μM SrtA were incubated for 3 hours at 37 °C and analysed by non-reducing SDS-polyacrylamide gel electrophoresis through 12% tris/glycine gels (Invitrogen, Australia). Rhodamine immunofluorescence was measured at 605 nm using a VersaDoc™ MP Imaging System. Where required, rhodamine-labelled proteins were purified by removal of unlabelled protein and SrtA from the reaction mixture using small-scale His-tag and Flag-tag pull-down purification (Ni-NTA superflow, QIAGEN; in house anti-FLAG monoclonal antibody resin[40]). Proteins were stored in small aliquots at 4 °C prior to use.

Cell-based immunofluorescence assays

Murine primary neuronal cells were isolated as previously described[41] from E14–16 embryos with approval from the Animal Ethics Committee of the Florey Institute of Neuroscience and Mental Health (Melbourne, Victoria, Australia). Neuronal cells were plated (6.5×10^4 cells cm^{-2}) on coverslips (ProSciTech, Kurwan, Queensland, Australia, coverglass no.1, 13 mm diameter) coated with poly-D-lysine (10 μg cm^{-2}, Sigma-Aldrich, St. Louis, MO) and incubated at 37 °C for 8–10 days *in vitro* (DIV). Cultures were fixed with ice-cold acetone for 15 min, then rinsed in PBS (non-permeabilising fixative such as paraformaldehyde was not used because the free aldehydes bind non-specifically to the rhodamine leading to high fluorescence background). Before labelling, the coverslips were treated with blocking buffer (2% w/v bovine serum albumin in 1× PBS) for 1 h at room temperature. The blocking solution was removed and replaced with PBS containing either Im7-LPETG-rhodamine (15 μM) or $A\beta_{1-42}$-Im7-LPETG-rhodamine (7.5 μM). After an overnight incubation at room temperature, the rhodamine proteins were removed and the coverslips were washed in 1× PBS for 5 min for a total of three washes. The nuclei were stained with 4′,6-diamidino-2-phenylindole (1 mg mL^{-1}, DAPI) in PBS for 10 min at room temperature. The coverslips were washed in 1× PBS for 5 min for a total of three washes. Coverslips were mounted onto slides with fluorescent mounting medium (Dako, Carpenteria, CA). Micrographs were captured using a fluorescence microscope (BX60, Olympus, Tokyo, Japan) and a QICAM 12-bit mono cooled camera (QImaging, Surrey, British Columbia, Canada).

Abbreviations

SrtA	Sortase A from *Staphylococcus aureus*
Aβ	amyloid beta peptide residues 1–42
PBS	Phosphate-buffered saline
scFv	single chain variable fragment antibody
TAMRA	5/6-carboxytetramethylrhodamine

Competing interests

The authors declare no competing interests.

Authors contribution

SB, LH, & CW synthesised rhodamine compounds and performed conjugation assays. JN & RN performed the neuronal imaging studies. MM, RS, & SN cloned and produced recombinant proteins and performed conjugation assays. GC & TA participated in the design of study and helped to draft the manuscript. CW & SN designed the experiments, conceived the

research and wrote the manuscript. Final manuscript was read and approved by all the authors.

Acknowledgements

We thank Mr Nick Bartone for performing the mass spectrometry and Dr Michael Bird for animal handling and obtaining the murine embryos.

References

1 P. J. Carter and P. D. Senter, *Cancer J.*, 2008, **14**, 154–169.
2 S. C. Alley, N. M. Okeley and P. D. Senter, *Curr. Opin. Chem. Biol.*, 2010, **14**, 529–537.
3 J. M. Reichert and E. Dhimolea, *Drug Discovery Today*, 2012, **17**, 954–963.
4 S. Webb, *Nat. Biotechnol.*, 2013, **31**, 191–193.
5 A. A. Wakankar, M. B. Feeney, J. Rivera, Y. Chen, M. Kim, V. K. Sharma and Y. J. Wang, *Bioconjugate Chem.*, 2010, **21**, 1588–1595.
6 G. D. Lewis Phillips, G. Li, D. L. Dugger, L. M. Crocker, K. L. Parsons, E. Mai, W. A. Blattler, J. M. Lambert, R. V. Chari, R. J. Lutz, W. L. Wong, F. S. Jacobson, H. Koeppen, R. H. Schwall, S. R. Kenkare-Mitra, S. D. Spencer and M. X. Sliwkowski, *Cancer Res.*, 2008, **68**, 9280–9290.
7 H. Ton-That, S. K. Mazmanian, K. F. Faull and O. Schneewind, *J. Biol. Chem.*, 2000, **275**, 9876–9881.
8 S. K. Mazmanian, G. Liu, H. Ton-That and O. Schneewind, *Science*, 1999, **285**, 760–763.
9 G. K. Paterson and T. J. Mitchell, *Trends Microbiol.*, 2004, **12**, 89–95.
10 A. P. Hendrickx, J. M. Budzik, S. Y. Oh and O. Schneewind, *Nat. Rev. Microbiol.*, 2011, **9**, 166–176.
11 E. M. Weiner, S. Robson, M. Marohn and R. T. Clubb, *J. Biol. Chem.*, 2010, **285**, 23433–23443.
12 N. Suree, C. K. Liew, V. A. Villareal, W. Thieu, E. A. Fadeev, J. J. Clemens, M. E. Jung and R. T. Clubb, *J. Biol. Chem.*, 2009, **284**, 24465–24477.
13 L. A. Marraffini, A. C. Dedent and O. Schneewind, *Microbiol. Mol. Biol. Rev.*, 2006, **70**, 192–221.
14 S. Tsukiji and T. Nagamune, *ChemBioChem*, 2009, **10**, 787–798.
15 T. Proft, *Biotechnol. Lett.*, 2010, **32**, 1–10.
16 J. G. Bolscher, M. J. Oudhoff, K. Nazmi, J. M. Antos, C. P. Guimaraes, E. Spooner, E. F. Haney, J. J. Garcia Vallejo, H. J. Vogel, W. Van't Hof, H. L. Ploegh and E. C. Veerman, *FASEB J.*, 2011, **25**, 2650–2658.
17 H. T. Ta, S. Prabhu, E. Leitner, F. Jia, D. von Elverfeldt, K. E. Jackson, T. Heidt, A. K. Nair, H. Pearce, C. von Zur Muhlen, X. Wang, K. Peter and C. E. Hagemeyer, *Circ. Res.*, 2011, **109**, 365–373.
18 M. W. Popp, S. K. Dougan, T. Y. Chuang, E. Spooner and H. L. Ploegh, *Proc. Natl. Acad. Sci. U. S. A.*, 2011, **108**, 3169–3174.
19 X. Huang, A. Aulabaugh, W. Ding, B. Kapoor, L. Alksne, K. Tabei and G. Ellestad, *Biochemistry*, 2003, **42**, 11307–11315.
20 T. Ito, R. Sadamoto, K. Naruchi, H. Togame, H. Takemoto, H. Kondo and S. I. Nishimura, *Biochemistry*, 2010, **49**, 2604–2614.
21 M. W. Popp and H. L. Ploegh, *Angew. Chem., Int. Ed.*, 2011, **50**, 5024–5032.
22 J. M. Antos, G. L. Chew, C. P. Guimaraes, N. C. Yoder, G. M. Grotenbreg, M. W. Popp and H. L. Ploegh, *J. Am. Chem. Soc.*, 2009, **131**, 10800–10801.
23 M. W. Popp, J. M. Antos and H. L. Ploegh, *Curr. Protoc. Protein Sci.*, 2009, **56**, 15.3.1–15.3.9.
24 R. Parthasarathy, S. Subramanian and E. T. Boder, *Bioconjugate Chem.*, 2007, **18**, 469–476.
25 R. M. Nisbet, S. D. Nuttall, R. Robert, J. M. Caine, O. Dolezal, M. Hattarki, L. A. Pearce, N. Davydova, C. L. Masters, J. N. Varghese and V. A. Streltsov, *Proteins*, 2013, **81**, 1748–1758.
26 M. P. Madej, G. Coia, C. C. Williams, J. M. Caine, L. A. Pearce, R. Attwood, N. A. Bartone, O. Dolezal, R. M. Nisbet, S. D. Nuttall and T. E. Adams, *Biotechnol. Bioeng.*, 2012, **109**, 1461–1470.
27 C. L. Masters and D. J. Selkoe, *Cold Spring Harb. Perspect Med.*, 2012, **2**, a006262.
28 I. Benilova, E. Karran and B. De Strooper, *Nat. Neurosci.*, 2012, **15**, 349–357.
29 J. M. Budzik, S. Y. Oh and O. Schneewind, *J. Biol. Chem.*, 2009, **284**, 12989–12997.
30 J. M. Budzik, S. Y. Oh and O. Schneewind, *J. Biol. Chem.*, 2008, **283**, 36676–36686.
31 S. Samantaray, U. Marathe, S. Dasgupta, V. K. Nandicoori and R. P. Roy, *J. Am. Chem. Soc.*, 2008, **130**, 2132–2133.
32 H. Decker, S. Jurgensen, M. F. Adrover, J. Brito-Moreira, T. R. Bomfim, W. L. Klein, A. L. Epstein, F. G. De Felice, D. Jerusalinsky and S. T. Ferreira, *J. Neurochem.*, 2010, **115**, 1520–1529.
33 R. D. Johnson, J. A. Schauerte, K. C. Wisser, A. Gafni and D. G. Steel, *PLoS One*, 2011, **6**, e23970.
34 F. M. LaFerla, K. N. Green and S. Oddo, *Nat. Rev. Neurosci.*, 2007, **8**, 499–509.
35 L. Zheng, A. Cedazo-Minguez, M. Hallbeck, F. Jerhammar, J. Marcusson and A. Terman, *Transl. Neurodegener.*, 2012, **1**, 19.
36 D. P. Virok, D. Simon, Z. Bozso, R. Rajko, Z. Datki, E. Balint, V. Szegedi, T. Janaky, B. Penke and L. Fulop, *J. Proteome Res.*, 2011, **10**, 1538–1547.
37 A. Patel and T. K. Lindhorst, *Carbohydr. Res.*, 2006, **341**, 1657–1668.
38 B. R. Matthews, G. Holan, P. Karellas, S. A. Henderson and D. F. O'Keefe, Agent for the prevention and treatment of sexually transmitted diseases-I, *US*, 2009/0269298, 2009.

39 S. M. Juraja, T. D. Mulhern, P. J. Hudson, M. K. Hattarki, J. A. Carmichael and S. D. Nuttall, *Protein Eng. Des. Sel.*, 2006, **19**, 231–244.
40 S. D. Nuttall, K. S. Humberstone, U. V. Krishnan, J. A. Carmichael, L. Doughty, M. Hattarki, A. M. Coley, J. L. Casey, R. F. Anders, M. Foley, R. A. Irving and P. J. Hudson, *Proteins*, 2004, **55**, 187–197.
41 R. M. Nisbet, J. Nigro, K. Breheney, J. Caine, M. K. Hattarki and S. D. Nuttall, *Protein Eng. Des. Sel.*, 2013, **26**, 571–580.